CHAPTER 5

Green synthesis of fluorescent carbon quantum dots for the detection of mercury (II) and glutathione

5.1. Introduction

Heavy metal toxicity has become a serious problem worldwide, which affects human health and the environment. Mercury is a hazardous heavy metal pollutant, which can bioaccumulate in the human body and flora and fauna and cause serious health disorders and ecological toxicity, respectively. It is a well-established fact that Hg^{2+} can simply pass through the skin and tissues, which leads to damage in the central nervous system and DNA and mitosis impairment [Gutknecht *et al.* (1981), Yan *et al.* (2014)]. Due to its non-biodegradable nature, it can only be diluted, but not destroyed [Yan *et al.* (2014)]. Therefore, it is necessary to develop an efficient analytical method for the sensitive detection of Hg^{2+}. The conventional techniques including auger electron spectroscopy (AES), polarography, and inductively coupled plasma mass spectroscopy (ICPMS) involve sophisticated and expensive instrumentations which limit their realistic applicability [Lu *et al.* (2012)].

The fluorescence-based assay has been proven as an alternative method to detect Hg^{2+} which have several advantages such as economical, high sensitivity, less cell-damaging, and fast analysis [Lu *et al.* (2012)]. Numerous fluorescent probes have been fabricated for the Hg^{2+} detection including metal nano-clusters, fluorescent dyes, semiconductor quantum dots, etc. Gong *et al.*, designed a fluorescent probe for the Hg^{2+} detection based on the rhodamine thiospirolactam derivative [Gong *et al.* (2012)]. Jiang *et al.* described ratiometric sensing of Hg^{2+} by using a cysteine functionalized gold nanoparticles [Jiang *et al*. (2011)]. Long *et al*., reported the strategy towards the Hg^{2+} detection by fluorescence of a CdS-encapsulated DNA nano-composite [Long *et al*. (2009)]. Lin et al., fabricated Hg^{2+} sensing probe based on lysozyme type VI-stabilized gold nanoclusters [Lin *et al.* (2010)]. However, these fluorescent

materials are subjected to the use of hazardous dye, toxic metal, and costly reagents. So, the development of facile economical and non-toxic route is highly desired towards the fluorescent materials.

Fluorescent carbon quantum dots (CQDs) having size 1−10 nm is a good alternative to the traditional heavy metal QDs because of its biocompatibility, easy preparation, low cytotoxicity, higher photo-stability, aqueous water solubility, wavelength tunable emission, functionalization, and environmental friendliness [Baker & Baker (2010), Shen *et al.* (2012)]. Various efforts have been made in the synthesis process to improve the functionality and optical properties of CQDs including laser ablation, arc discharge, chemical oxidation, electrochemical oxidation, hydrothermal carbonization, and microwave irradiation [Huang *et al.* (2014), He *et al.* (2015), Cao *et al.* (2007), Zhou *et al.* (2007), Wang *et al.* (2011), Zhu *et al.* (2009)]. Amongst these processes, laser ablation and arc discharge need sophisticated and expensive appliance whereas the chemical oxidation and electrochemical oxidation needs very strong acid. Microwave irradiation provides an easy pathway to synthesize the CQDs within few minutes which is limited by the uncontrollable reaction conditions. At present, the hydrothermal route is frequently preferred because this method provides simplicity, rapidity, controlled reaction conditions, and cost-effectiveness [Alam *et al.* (2015)]. There are many organic compounds that have been used for the synthesis of CQDs such as glycol, glucose, sucrose, chitosan, and glycerol [Alam *et al.* (2015)]. For the surface passivation, a large number of organic polymeric moieties have been frequently used such as polyethyleneimine, polyethylene glycol, and 4,7,10-trioxa-1,13-tridecanediamine [Sachdev *et al.* (2015)]. Use of organic chemicals, strict reaction condition, and post surface passivation are complicated and hence limited their applications [Alam *et al.* (2015)].

Hence taking into account of all the factors, the green route has been highly attractive for the synthesis of CQDs, which develop the use of natural renewable carbon sources. The uses of green sources have several advantages due to zero cost, non-toxicity, clean and easy availability. There are already reported literatures where the natural green sources such as soybean, pomelo peel, orange juice, green grass, milk, potato, plant leaves, soy milk, and cocoon silk have been used to the synthesis of CQDs [Li *et al.* (2013), Lu *et al.* (2012), Sahu *et al.* (2012), Liu *et al.* (2012), Lu *et al.* (2013), Lu *et al.* (2017), Zhu *et al.* (2012), Li *et al.* (2013). Nevertheless, the key challenge remains to develop the CQDs up to the high quantum yield (QY) amounts by using simple, straight, and one-step methodologies.

Herein; we have reported a green synthetic approach towards the synthesis of CQDs from a *Tamarindus indica* (T. *indica*) leaves by a simple one-step hydrothermal method. This methodology takes zero-cost, less time and double distilled water used as a reaction solvent. There is no need for the additional surface passivating reagent as *T. Indica* leaves serve as carbon precursors as well as a surface passivating agent. These leaves are the fair resource of the Vitamin-C, protein, and carbohydrates which are plentiful in carbon, oxygen, and nitrogen.[25] Consequently, CQDs are synthesized by a simple hydrothermal treatment involving polymerization, dehydration and carbonization step. The synthesized CQDs show blue luminescent at λ_{ex} = 365 nm under a UV light. Several physicochemical and optical properties have also been investigated in the present work. Apart from this, the synthesized CQDs can also serve as selective detection of Hg^{2+} with a minimum limit of detection (LOD) via electron transfer process. Since the Hg^{2+} have a high binding capacity with sulfur atom through the Hg-S bond formation. By using this property CQDs/Hg^{2+} could act as another sensor for the glutathione (GSH) with good selectivity.

5.2. Materials and method

5.2.1. Synthesis of CQDs

Typically in a given experiment 4 g *T. indica* leaves was taken, collected from the campus area of IIT (BHU), and washed it several times with the ultrapure distilled water. Then it was finely cut into a very small pieces and dissolved into a 100 mL of distilled water in a beaker and transferred into a 250 mL of Teflon-lined autoclaved and kept it for 5 hours at 210 ºC. The obtained solution was cooled down to room temperature (RT) naturally. The black-brown carbonaceous material was centrifuged up to 10,000 rpm to remove the larger particles. And then obtained solution was purified against the dialysis membrane for 2-3 days (3.5 KDa). The concentration of purified CQDs adjusted to the 0.4 mg mL^{-1} using the hot air oven at 50 ºC for further characterizations and use.

5.2.2. Assay for the detection of Hg^{2+}

All the experiment is performed in a sodium acetate buffer (Na-Ac) (0.2 M, pH 7) at RT. Typically 100 μL of the synthesized CQDs is maintained in a one mL of Na-Ac buffer followed by the calculated amount of the Hg^{2+}. The corresponding FL emission spectra are recorded after the reaction intended for 5 min. Sensitivity and selectivity of the detecting system are calculated in triplicate.

5.2.3 Experimental methodology

The synthesized CQDs were characterized by a variety of spectroscopic techniques. UV-Visible absorbance spectra were recorded by Thermo Scientific, Evolution 301 Spectrophotometer. Fluorescence emission spectra were recorded by Varian CaryEclipse Fluorescence Spectrophotometer. Size and shape were measured by Transmission Electron

Microscopy (TEM, TECHNAI G^2 20 S–TWIN). X-Ray Diffractometer (XRD) spectra were recorded by Rigaku MiniFlex 600, having Cu Kα radiation source and Ni filter at a scanning rate of 3° min^{-1}. The functional groups were explored by using the Fourier Transform Infrared Spectrophotometer (FTIR, Perkin Elmer Spectrum 100). The chemical compositions were identified by the X-Ray Photoelectron Spectroscopy (XPS, AMICUS, Kratos Analytical, A Shimadzu). The fluorescence decay measurements were carried out by using Edinburgh Instrument.

5.2.4. Quantum yield determination

The quantum yield of the synthesized CQDs was measured in reference to quinine sulphate from the given **equation 2.3** mentioned in **chapter 2** in a **section 2.6.1**.

5.3. Results and discussion

5.3.1. Characterizations

CQDs are prepared from the *T. indica* leaves by simple one-step hydrothermal treatment at 210 °C for a period of 5 h (**Scheme 5.1**).

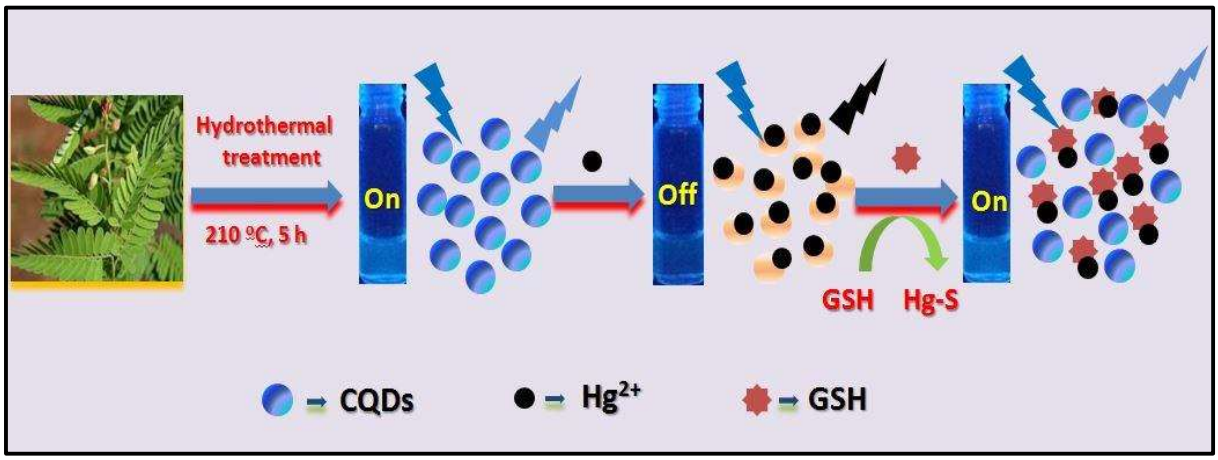

Scheme 5.1 Representation of one-step synthesis of CQDs for the detection of Hg^{2+} and GSH.

Figure 5.1a shows the typical TEM micrograph of CQDs which reveals the abundance of mono-disperse spherical nanoparticles. **Inset figure 5.1a** is showing the size distribution histogram corresponding to TEM micrograph which represents that the maximum CQDs were in the range of 3 to 3.5 nm by counting 34 particles with an average calculated size 3.4 ± 0.5 nm. Figure 5.1b represents the typical SAED micrograph of the CQDs. Broad circular rings in a SAED pattern reveals that the prepared CQDs is amorphous. The crystalline nature of the as-prepared CQDs is confirmed by an XRD analysis. The XRD spectrum showed a broad peak at 2θ = 22° which is attributed to the 002 Bragg reflection as shown in **Figure 5.1c**. The interlayer spacing corresponding to this plane is equal to 0.32 nm which is similar to the graphitic interlayer spacing and consistent with the above SAED result. This result indicates that the prepared CQDs is amorphous and graphitic [Lin *et al.* (2015), Hsu *et al.* (2012)]. The FTIR analysis reveals the functional group present on the CQDs surface. **Figure 5.1d** presents the characteristic peaks at 3427 cm^{-1}, 1340 cm^{-1}, and 1659 cm^{-1}. The peaks at 3427 cm^{-1} assigned to the -OH/-NH whereas the peak 1340 cm^{-1}, 1650 cm^{-1} ascribed to the O=C–NH- and conjugated C=C stretching vibration in an aromatic heterocyclic ring [Dong *et al.* 2012, Yu *et al.* (2016)].

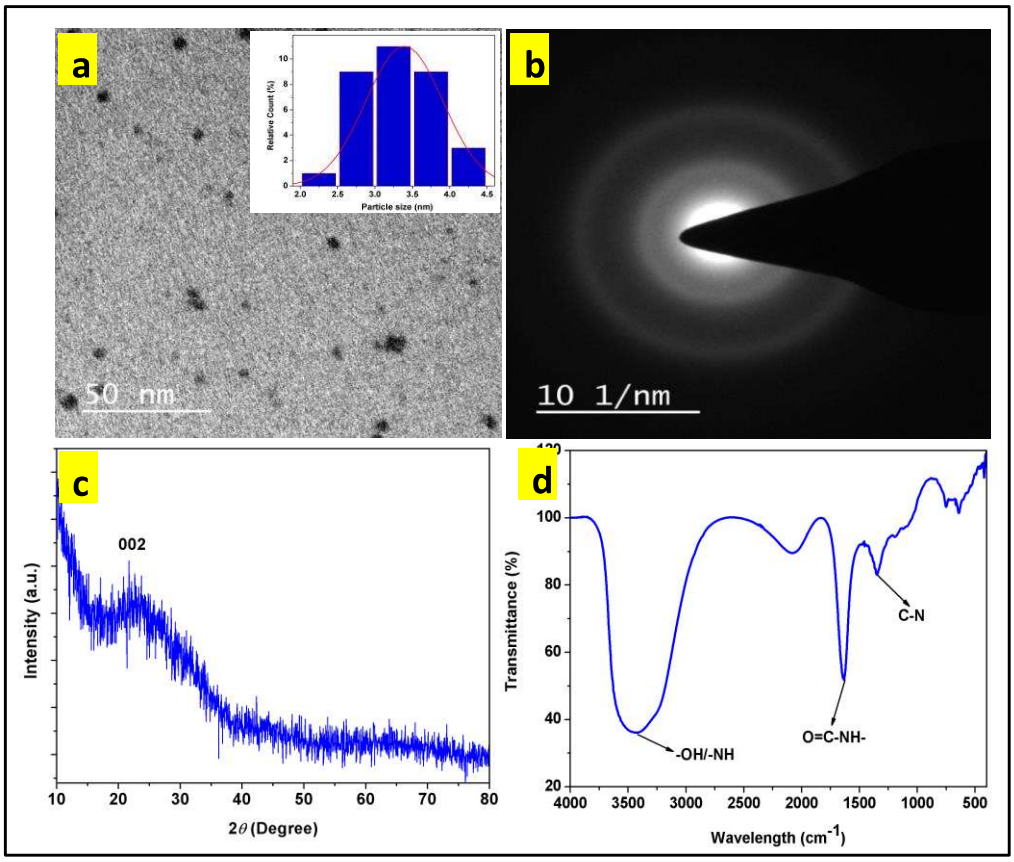

Figure 5.1 (a) Representing the TEM micrograph of CQDs whereas inset shows the size distribution by counting 34 particles, (b) SAED micrograph of CQDs, (c) XRD spectrum of CQDs at scan rate 3°/min in a range 10-80°, (d) FTIR spectrum of the as-prepared CQDs in a range 400-4000 cm^{-1}.

The XPS measurements are carried out to classify the chemical composition and bond present on the surface of CQDs **(Figure 5.2)**. The wide range XPS spectra (**Figure 5.2a**) of the CQDs shows the characteristics peak of 284.6 eV, 400 eV, and 531 eV which confirms the C (51.1 %), N (14.2 %), and O (34.7 %) were the major constituents of the prepared CQDs. The C 1s spectrum (**Figure 5.2b**) reveals the occurrence of four peak at 284.6 eV, 285.7 eV, 286.6 eV, and 287.8 eV which is due to the presence of C–C, C=C, C–O/C–N, and C=O bond.[22, 30] The N 1s spectrum explores the three peak centered at 399.3 eV, 400.7 eV,

and 401.6 eV which is due to the C–N–C, N–C_3 and N–H bond, respectively **(Figure 5.2c)** [Lin *et al*. (2015), Liu *et al.* (2012)]. The O 1s spectrum indicates the presence of two peaks at 531.6 eV and 533.0 eV which is owing to the presence of C=O and C–OH/C–O–C respectively [Lu *et al.* (2012)]. This result consistent with the result obtained from the FTIR which indicates the presence of amide groups and a hydroxyl group in the CQDs structure (**Figure 5.2d**).

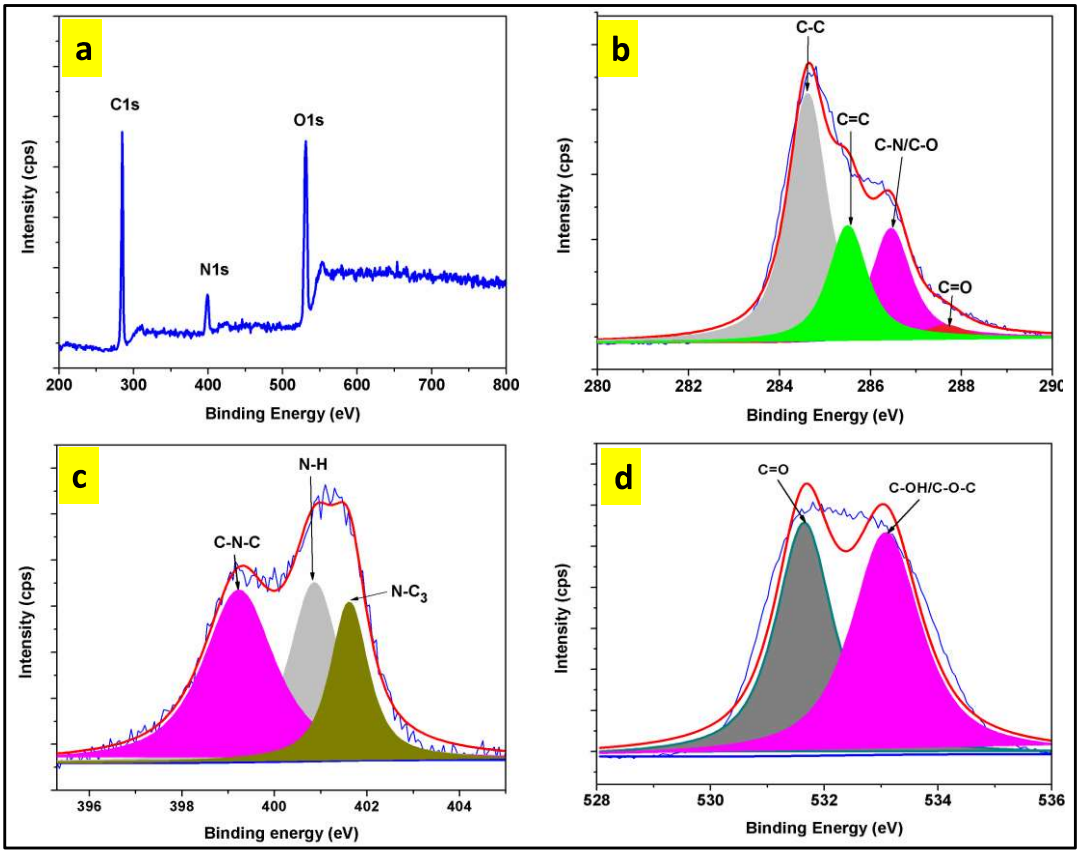

Figure 5.2 (a) Full scan XPS spectrum of CQDs, (b) shows the C 1s spectrum, (c) N 1s spectrum, and (d) O 1s spectrum of CQDs.

5.3.2. Optical Properties

Figure 5.3a shows the UV-visible (black line) and Fluorescence (FL) emission spectra (blue line) of prepared CQDs. Inset **figure 5.3a** shows the synthesized CQDs exhibit the blue color emissions under the UV excitation of 365 nm in a UV chamber. This result shows the prepared CQDs is fluorescent. From the dispersion of CQDs a single absorption peak is observed which is centered at 280 nm which is ascribed to the π-π* electronic transition of C=C and emission peak is obtained at 433 nm at 365 nm excitation. **Figure 5.3b** shows that the prepared CQDs exhibit excitation dependent behavior in the range 260-400 nm with the difference of 20 nm. This result confirms that the prepared CQDs have a different emissive trapped surface state for the fluorescence emission.

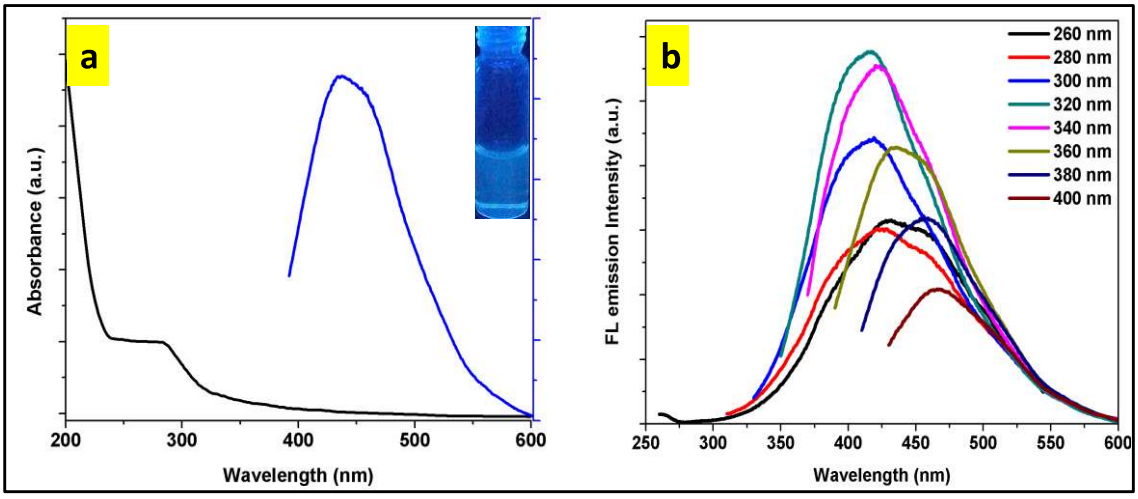

Figure 5.3 (a) Represents the UV-visible spectrum (black)) and emission intensity spectrum (blue) at λ_{ex} of 360 nm of N-CQDs whereas inset showing the photograph of vial under UV excitation 365 nm, (b) represents the emission intensity at different excitation wavelength (260, 280, 300, 320, 340, 360, 380, 400 nm).

The mechanism responsible for the blue fluorescence of CQDs is still debatable. The earlier literatures report that the isolated sp^2 clusters having a size less than 10 nm within the carbon-oxygen matrix can yield band gaps which are consistent with the blue fluorescence emission due to the localization of electron-hole pairs [Eda *et al.* (2010)]. Thus, in addition to the size and surface effects, the presence of oxygen-rich group and more electron withdrawing nitrogen atoms play the significant role to the observed blue shift in fluorescence emission of CQDs [Lin *et al.* (2015)]. To further explore the fluorescent properties of the prepared CQDs, the QY and the irrelevant factor which affect the emission of CQDs is investigated. The QY of the as-prepared CQDs is found to be 46.6 % under the λ_{ex} of 360 nm by using quinine sulfate (in a 0.1 M H_2SO_4, QY = 0.54) as a standard (**Table 5.1**). Since the photoluminescence of CQDs is still under study, hence we have calculated relatively high QY illustrated by the results obtained from the FTIR and XPS analysis. The occurrence of hydroxyl and amide group can efficiently enhance the intrinsic state emissions by suppressing the non-radiative electron-hole pairs recombination [Zhu *et al.* (2012)]. As a result, the photoluminescence and QY of the CQDs is increased sharply. The stability is also investigated under various physiological conditions. There is no remarkable fluorescence change is observed after incubating the sample for 5 months at 4 ºC **(Figure 5.4a)**. This finding confirms that the prepared CQDs are highly stable and more disperse. The stability of CQDs under the high ionic strength is also checked by adding the different concentration of NaCl (0–50 mM) **(Figure 5.4b)**. It is observed that the fluorescence remains unchanged on adding the NaCl concentrations. This result confirms that the prepared CQDs are stable and did not aggregate even under high ionic strength conditions and could be potentially applied for the sensing and several other analytical applications.

Table 5.1 Quantum yield of CQDs with respect to Quinine sulfate.

Sample	Integrated emission intensity at λ_{ex} = 360 nm	Absorption at 360 nm	QY (%)
Quinine sulfate	68430.2	0.04	54.0
CQDs	44635.9	0.03	46.6

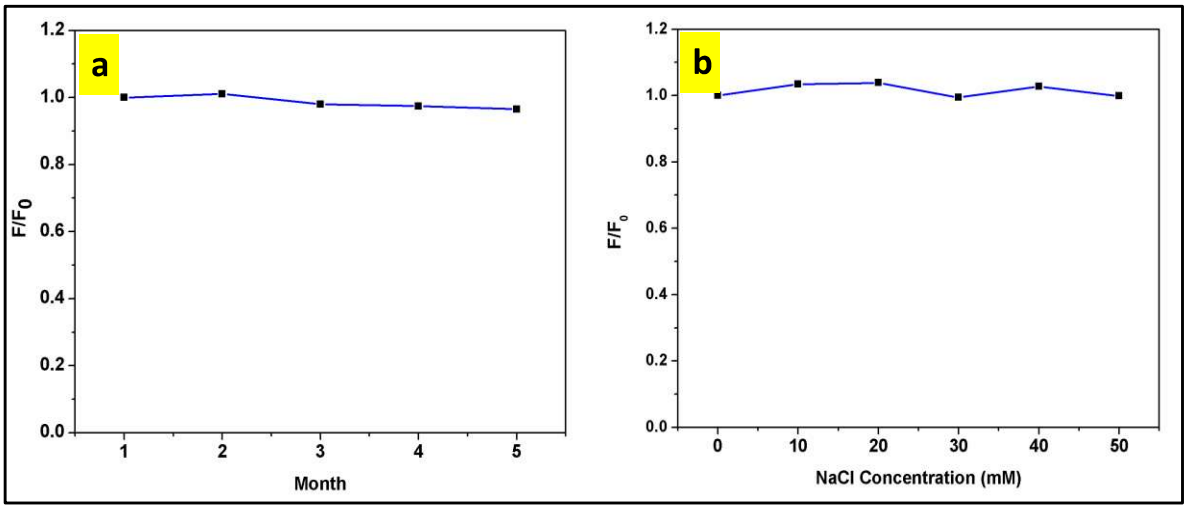

Figure 5.4 (a) Photostability of CQDs, showing the fluorescence of CQDs remain almost same even after incubating 5 months at 4 °C, (b) stability under the high ionic strength after the addition of different concentration of NaCl (0, 10, 20, 30, 40, 50 mM).

5.3.3. Fluorescence strategy towards the Hg^{2+} detection

5.3.3.1. Optimization of experimental conditions towards the Hg^{2+} detection

To achieve the sensitivity of present CQDs based nano-probe towards the Hg^{2+} detection, pH is optimized in the range 3 to 13. We examined that only slight change is observed in FL emission intensity of CQDS as shown in **Figure 5.5a**. This result indicates that the present sensing system is insensitive to the pH. Hence we will analyze the sensing experiment at pH 7. Furthermore the optimum time of the present sensing system is also

investigated. The kinetic characteristic of this sensing system at different time interval is investigated by the addition of 50 μM of Hg^{2+} concentration in CQDs. From the **Figure 5.5b,** it is clear that a stable fluorescence emission is obtained which is centered at 433 nm within a reaction time of 5 min. This result is indicating that only 5 min incubation time is optimum to complete the quenching process. Hence after optimizing the experimental conditions, an outstanding fluorescence sensing probe is developed for the Hg^{2+} detection.

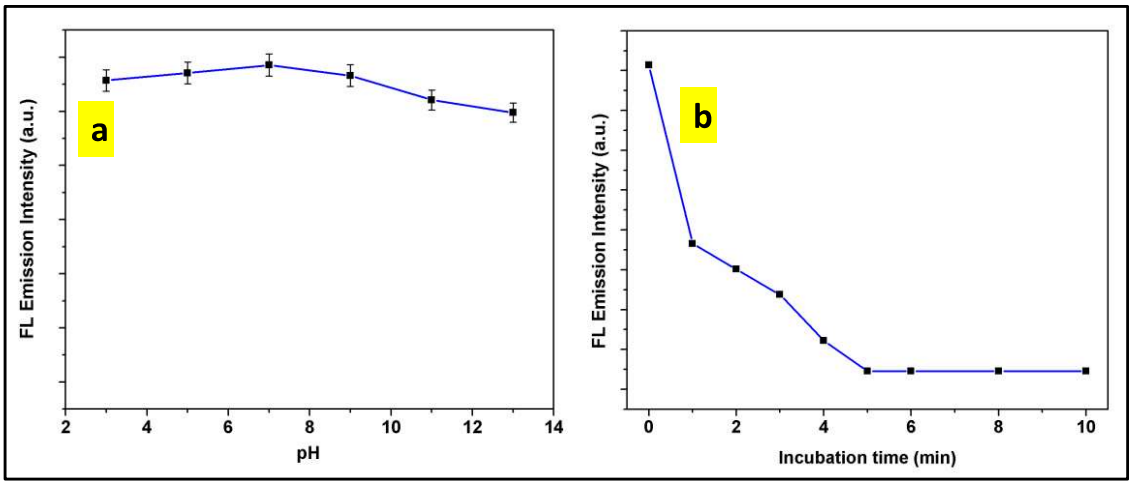

Figure 5.5 (a) Represents the optimization of pH ranges from 3 to 13, showing that prepared CQDs is independent of the pH used, (b) the kinetic stability of CQDs-Hg^{2+} system, indicating 5 min time is optimum to complete the quenching mechanism.

5.3.3.2. Selectivity towards the detection of Hg^{2+}

The selectivity is an important parameter to assess the sensing performance. For this purpose, we examine the change in FL emission intensity by adding various environmentally and biologically relevant metal ions including Al^{3+}, Zn^{2+}, Hg^{2+}, Pb^{2+}, Cd^{2+}, Ca^{2+}, Mg^{2+}, Cu^{2+}, Ni^{2+}, Fe^{2+}, and Fe^{3+} ions of 50 μM into the CQDs solution and the corresponding FL emission spectra is recorded. From the **Figure 5.6,** it is clear that most of the ions have

negligible effect in emission except Hg^{2+}. **Inset figure 5.6** is showing the photograph of vials under UV excitation which reveals that the highly selective fluorescence quenching is observed in case of Hg^{2+}.

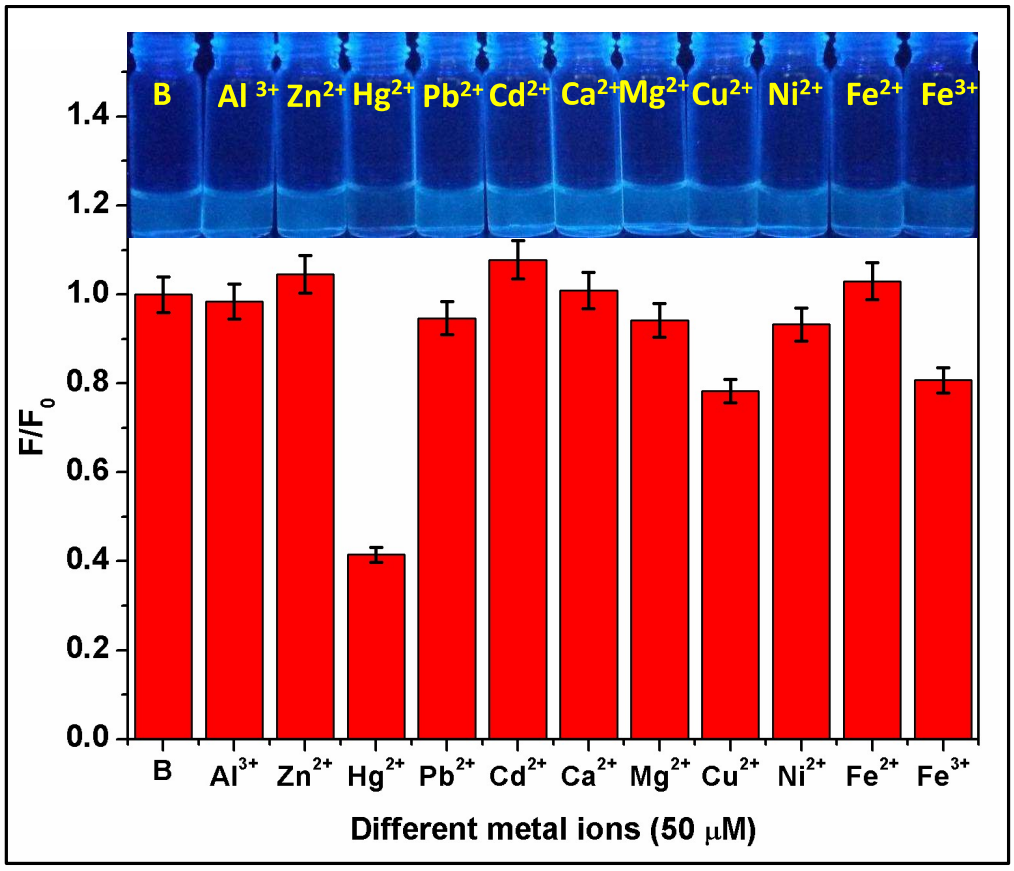

Figure 5.6 Change in FL emission intensity of CQDs solution (0.4 mg/L) at λ_{ex} = 360 nm in the presence of 50 μM various metal ions including (Al^{3+}, Zn^{2+}, Hg^{2+}, Pb^{2+}, Cd^{2+}, Ca^{2+}, Mg^{2+}, Cu^{2+}, Ni^{2+}, Fe^{2+}, and Fe^{3+}), whereas inset showing the photographs of vials under a UV excitation of 365 nm (F and F_0 are the emission intensities of CQDs with the presence and absence of different metals).

Figure 5.7a presents the FL life time spectra of CQDs in the absence and presence of Hg^{2+}. It is seen that the addition of 50 μM Hg^{2+} decreases the lifetime (5.12 ns) from the uncontaminated CQDs lifetime (5.98 ns). Hence the decrease in lifetime indicating that the electron transfer amid the CQDs and Hg^{2+} which is reliable with the preceding reports [Lin *et al.* (2015). So, the quenching mechanism ascribed to the non-radiative electron transfer from the excited states of CQDs to the d-orbital of the Hg^{2+}. Furthermore, the performance of the proposed sensing system is also evaluated under the presence of different possible interference ions as shown in **Figure 5.7b**. Most of the ions do not effect and can be allowed to 100 times of the Hg^{2+} concentration. The Fe^{2+}, Cd^{2+}, Ni^{2+}, and Zn^{2+} have negligible effect on the detection and allowed to exist greater than 100 times. Cu^{2+} and Fe^{3+} ions have mild interference and kept the concentration 5 times less. Hence our CQDs based system is feasible and could acts as a nano-probe towards the selective detection of Hg^{2+}.

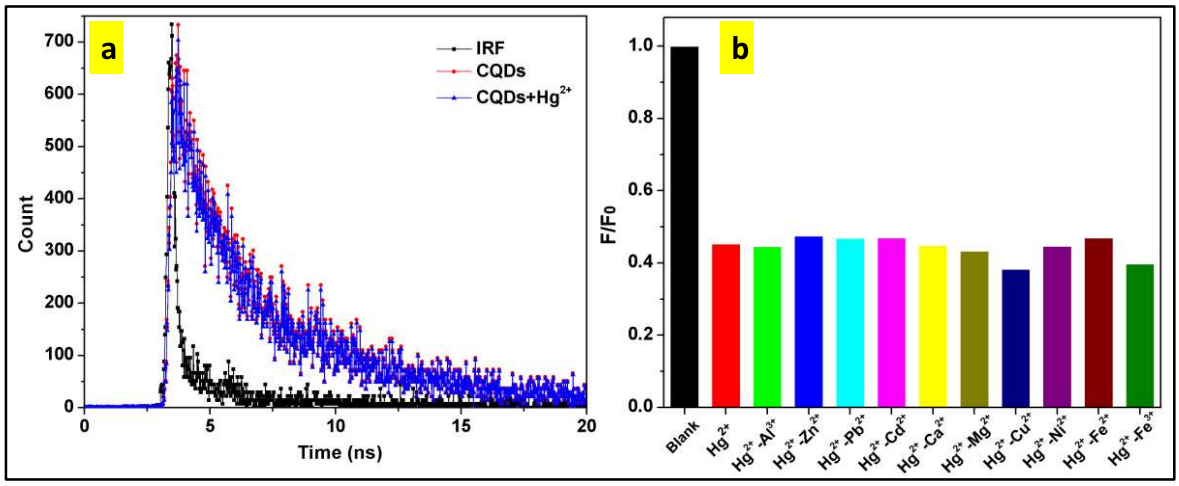

Figure 5.7 (a) Fluorescence decay curve for the Hg^{2+} detection analysis, (b) Interference study under various conditions [Hg^{2+}] = 0.05 mM, [Al^{3+}] = [Pb^{2+}] = [Ca^{2+}], [Mg^{2+}] = 5 mM, [Zn^{2+}] = [Cd^{2+}] = [Ni^{2+}] = [Fe^{2+}]= 10 mM, [Cu^{2+}] = [Fe^{3+}] = 0.01 mM.

5.3.3.3. Sensitivity towards the detection of Hg^{2+}

Accordingly, the sensitivity titration is also investigated under the different Hg^{2+} concentration in the range (0 to 50 μM) at pH 7. From the **Figure 5.8a,** it is clear that on increasing the concentration of Hg^{2+} emission at 433 nm of CQDs is gradually decreased which reveals that the present sensing system is highly sensitive to the Hg^{2+} concentration. A good linear relationship is obtained between the linear ranges at 0 to 0.1 μM with a correlation coefficient (R^2) is 0.997 as shown in **Figure 5.8b**. The LOD is found to be 6 nM with S/N ratio 3 and SV quenching constant is calculated to be 2 x 10^6 L/mol. According to Environmental Protection Agency, the maximal permissible limit of Hg^{2+} in drinking water is 10 nM (2 ppb) [Lu *et al.* (2012)]. This result indicates that our sensing probe is sensitive enough to detect Hg^{2+} concentration in drinking water. From the **Table 5.2,** it is seen that our sensing system is superior to other fluorescent nano-probe towards the of Hg^{2+} detection [Li

et al. (2011), Huang *et al.* (2007), Li *et al.* (2012), Zhou *et al.* (2012), Lu *et al.* (2012), Gonçalves *et al.* (2010), Zhang *et al.* (2014)].

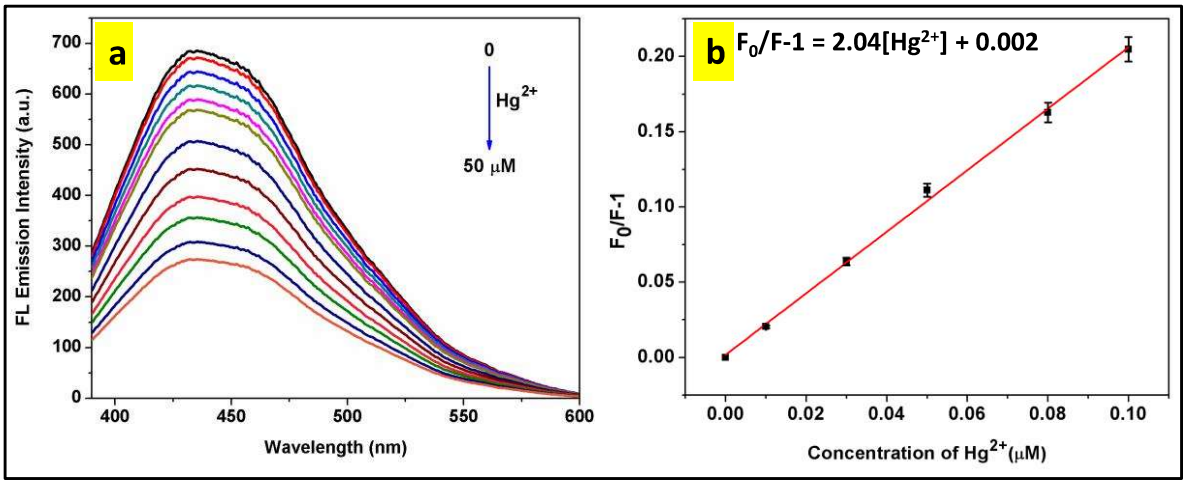

Figure 5.8 (a) Illustrating the FL emission intensity of CQD–Hg^{2+} system at 433 nm as a function of Hg^{2+} concentration, (b) represents the dependence of F_0/F-1 on the Hg^{2+} concentration within the linear range 0-0.1 μM. The error bar represents the standard deviation of three replicate measurements.

Table 5.2 Sensing performance of different fluorescent nano-probe towards the Hg^{2+} detection.

Fluorescent probe	QY (%)	Limit of detection (LOD)	Linear range	Ref.
Cd-Te quantum dots	-	1.55 nM	2–14 nM	[Li *et al.* (2011)]
Fluorescent gold nanoparticles	-	5 nM	1–10 x 10^4 nM	[Huang *et al.*(2007)]
Polymer sensor	-	0.728 μM	1–30 μM	[Li *et al.* (2012)]
Carbon dots (CDs)	11	4.2 nM	0–3 x 10^4 nM	[Zhou *et al.* (2012)]
Carbon Particles (CPs)	6.9	0.23 nM	0.5–10 nM	[Lu *et al.* (2012)]
Functionalized carbon dots	-	2.69 μM	0.1–2.69 μM	[Gonçalves *et al.*(2010)]
N-CQDs	15.7	0.23 μM	0–25 μM	[Zhang *et al.* (2014)]
CQDs	46.6	6 nM	0–0.1 μM	[Bano *et al.* (2019)]

5.3.3.4. Recovery experiment towards the GSH detection

It is found that on adding the GSH concentration into the CQDs/Hg^{2+} solution, the fluorescence got turn-on. Hence the CQDs/Hg^{2+} system can act as a turn on sensor towards the GSH detection. The selectivity of this sensing system has also been investigated by adding different amino acids into the CQDs/Hg^{2+} system. **Figure 5.9** is showing that the fluorescence recovery is obtained only in the case of GSH which reveal the CQDs/Hg^{2+} system is selective to glutathione in a given amino acids.

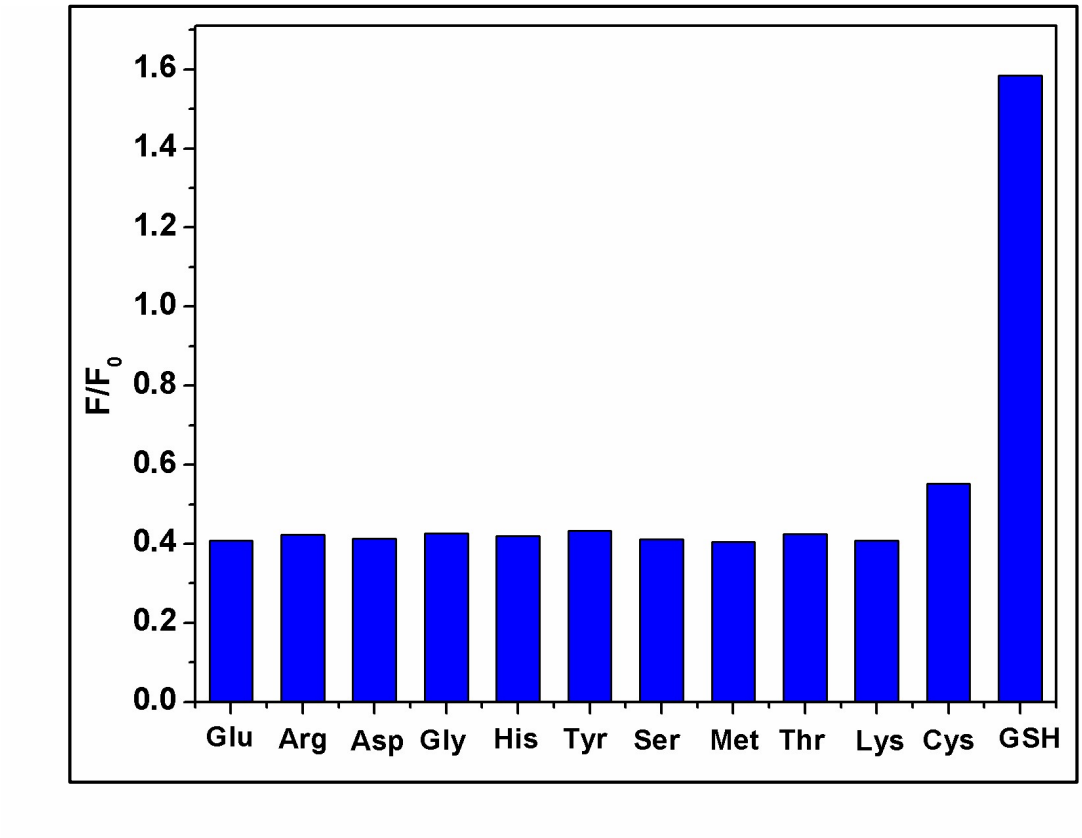

Figure 5.9 The fluorescence response of CQDs/Hg^{2+} solution towards different essential amino acids of concentration 40 µM where F and F_0 are fluorescence intensities of CQDs/Hg^{2+}/amino acid and CQDs respectively.

Figure 5.10a reveals that on increasing the concentration of glutathione from 0 to 40 µM, the fluorescence emissions of CQDs increased and quenched fluorescence got turn-on. **Figure 5.10b** showing the linear response between the range 0 to 20 µM with $R^2 = 0.984$ and the LOD towards the GSH detection is found to be 1.7 µM. The reappearance of fluorescence is due to the formation of Hg-S bond (soft-soft interaction) which leads to the elimination of Hg^{2+} from the CQDs surface.

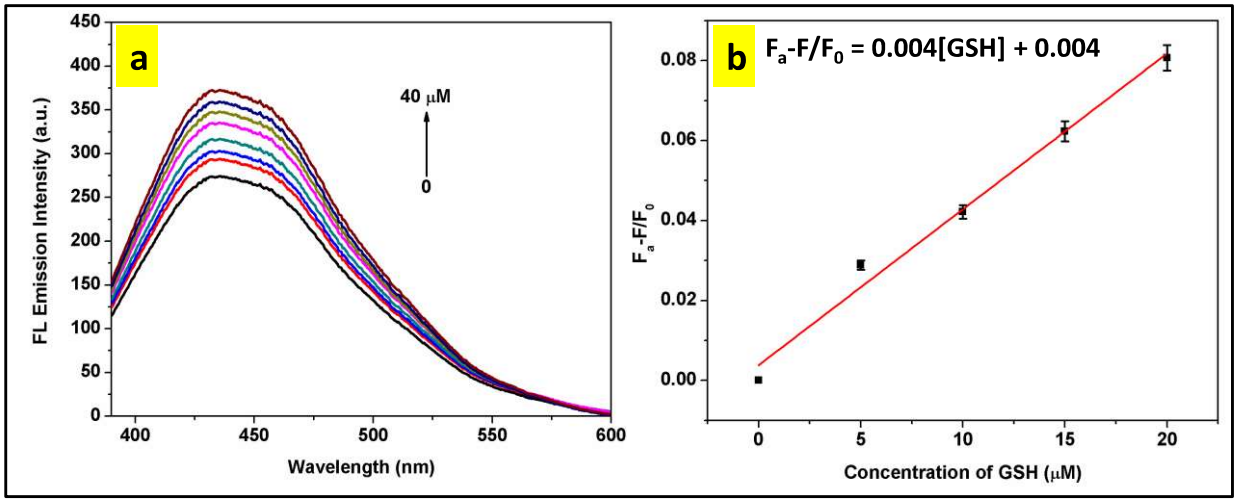

Figure 5.10 (a) FL spectra of CQDs/Hg^{2+} in the increasing concentration of GSH (0 to 40 μM), (b) showing relationship between FL of CQDs/Hg^{2+} and GSH from 0 to 20 μM. The error bars represent the standard deviation of three replicate measurements. Whereas F_a is the recovered emission intensity of CQDs in the presence of GSH, F is the FL intensity of CQDs in the presence of Hg^{2+} (50 μM), and F_0 is the emission of CQDs at 433 nm, respectively.

5.3.3.5. Detection of Hg^{2+} in natural sample

To check the realistic application, the feasibility of CQDs based nano-probe is explored in the real water sample by using pond water obtained from the IIT (BHU) campus at Varanasi, India. This water is filtered through a 0.22 μm membrane and centrifuged up to 10,000 rpm for 15 min. The obtained sample is spiked through the different concentration of Hg^{2+} (20, 50, and 70 nM). It is observed that the value is reliable with the Hg^{2+} added as shown in **Table 5.3**. The obtained recovery is in the range of 97-101 % and the relative standard deviation (RSD) for the three replicate measurements is less than from the 5%. This result indicates that the present approach is viable towards the Hg^{2+} detection in the natural water sample analysis.

Table 5.3 Detection of Hg^{2+} in natural water sample and RSD for n = 3.

Sample	Spiked Hg^{2+} (nM)	Measured (nM)	Recovery (%)	RSD (%)
Pond water	20	20.14	100.7	3.4
	50	49.70	99.4	2.2
	70	68.65	98.1	3.1

5.4. Conclusion

Herein; a green synthetic approach is developed for producing fluorescent CQDs by the hydrothermal treatment of *T. indica* leaves for the first time. Furthermore, the synthesized CQDs is prepared without any chemical modification which offers the advantages of cost-effectiveness and effortlessness. The as-prepared CQDs show excitation dependent behavior in the range 260–400 nm with a high QY of 46.6%. In addition, the prepared CQDs also served as a label-free sensing probe for the detection of Hg^{2+} which exhibits the high sensitivity and selectivity with a LOD as low as 6 nM in a linear range of 0 to 0.1 μM. Apart from this, the quenched system of CQDs/Hg^{2+} can act as a nanoprobe for the detection of glutathione selectively in a different amino acids. The feasibility of the proposed sensing system toward the detection of Hg^{2+} sensing system is also effectively used for the analysis of real pond water sample. Therefore, the present approach upwards the scalability in terms of producing bio-compatible CQDs which could be potentially applied in sensing, bio-imaging, disease diagnostics, and other analytical applications.